Bioluminescence Imaging of Carbon Monoxide in Living Cells and Nude Mice Based on Pd-Mediated Tsuji-Trost Reaction

Xiaodong Tian, Xinda Liu, Anni Wang, Choiwan Lau, and Jianzhong Lu

Anal. Chem., **Just Accepted Manuscript** • DOI: 10.1021/acs.analchem.8b01102 • Publication Date (Web): 11 Apr 2018

Bioluminescence Imaging of Carbon Monoxide in Living Cells and Nude Mice Based on Pd^0-Mediated Tsuji-Trost Reaction

Xiaodong Tian, Xinda Liu, Anni Wang, Choiwan Lau, and Jianzhong Lu*

School of Pharmacy, Fudan University, 826 Zhangheng Road, Shanghai 201203, China

Email: jzlu@shmu.edu.cn; Tel: 0086-021-51980058

ABSTRACT: Carbon monoxide (CO) is highly toxic and lethal to humans and animals because of its strong affinity for hemoglobin, while this "silent killer" is constantly generated in the body as a cell-signaling molecule of gasotransmitter family in various pathological and physiological conditions. Up to now, designing fluorescent probes for real-time imaging of CO in living species is a continuous challenge due to background interference, light scattering and photoactivation/photobleaching. Herein, a novel type of bioluminescence probe (allyl-luciferin) was synthesized and exploited to realize CO imaging with high signal-to-noise ratios. Based on Pd^0-mediated Tsuji-Trost reaction, allyl-luciferin specifically reacted with CO to yield D-luciferin and thus generate a turn-on bioluminescence response, exhibiting high selectivity against bioactive small molecules such as reactive nitrogen, oxygen and sulfur species. Furthermore, the new probe can be easily employed to detect exogenous CO in Huh7 cells and MDA-MB-231 cells, which exhibited CO production was enhanced greatly in these living cells after pre-treated with [$Ru(CO)_3Cl$-(glycinate)] (CORM-3). Through the use of $PdCl_2$-containing liposomes to improve poor membrane permeability of $PdCl_2$, endogenous CO stimulated by heme was also seen clearly. In addition, the probe was successfully used to monitor exogenous and endogenous CO in nude mice. Overall, our data proved that the allyl-luciferin is a promising tool for exogenous and endogenous CO detection and imaging within living species. This is the first demonstration of bioluminescence imaging obtained by a probe for CO. We anticipate that the good imaging properties of allyl-luciferin presented in this study will provide a potentially powerful approach for illuminating CO functions in the future.

INTRODUCTION

Carbon monoxide (CO) outcompetes oxygen when binding to the iron center of hemeproteins, leading to a reduction in blood oxygen level and acute poisoning. As we known, CO is highly toxic and lethal to humans and animals which are usually inhaled from common sources[1-2]. However, emerging studies showed that this "silent killer" is constantly generated in the body through the interaction of heme and heme oxygenase[3-6], similar to other two gasotransimitter molecules NO[7-11] and H_2S[12-19]. As a second gas messenger, the biological function of CO has been validated in modulating responses to both chemical and physiological processes such as anti-inflammatory response[20-21], vascular smooth muscle[22], neurotransmission[23-24], vasorelaxation[22] and antiproliferative activities[25-26]. However, its abnormal metabolism has a significant correlation with some severe diseases such as hypertension[3], Alzheimer`s disease[27], heart failure[28], etc.

Currently, a major barrier to further illuminate potential functions of CO is lack of ways for selectively tracking this transient small molecule within biological systems. Available techniques are limited for detecting CO, especially under living specimens, including electrochemical[29-30], colorimetric[31-33] and gas chromatography[34], etc. Significant effort has gone into the development of molecular imaging technologies and most approaches have revolved around optical imaging with a particular focus on fluorescence imaging. As we known, fluorescence is a common useful modality for optical imaging that is broadly used for detection and monitoring of various biological processes. Recently, several fluorescent probes have indeed been reported for the specific detection of CO in living cells [2-3, 29, 34-37], but their depth penetration of detection still need further improvement because of the inevitable interference of background fluorescence, light scattering and photoactivation/photobleaching[18].

Unlike fluorescence based assays, chemiluminescence (CL) and bioluminescence (BL) luminophores are considered as one of the most sensitive families of probes for detection and imaging applications, as no excitation light source is required and background signal is not affected by phenomena like autofluorescence[38-42]. Thus, it is imperative to develop CL/BL probes with high signal-to-noise ratios so as to eliminate the auto-interference. Based on these considerations, we first proposed to design and synthesize a novel type of BL probe that is capable of tracing CO in aqueous buffer and in biological systems. Recently we have developed a turn-on reaction-based BL probe for imaging H_2S[18] by taking advantage of its specific reduction ability. In contrast, CO is not a particularly electrophilic or nucleophilic reagent, and thus

we have to find a new approach to solve this problem. Herein we sought to employ one Pd^0-mediated Tsuji-Trost reaction for the development of a BL turn-on probe for CO detection. As depicted in Scheme 1, a novel BL probe allyl-luciferin was designed where one allyl ether substituent would cage the hydroxyl group of D-luciferin and thus hide its interaction with firefly luciferase and consequently quench BL emission. Meanwhile, the allyl ether is anticipated to be the reaction site that can be easily removed via Pd^0-mediated Tsuji-Trost reaction. Hence, we envisaged that this allyl ether-based probe would have the same mechanism for particular detection of CO [29, 35, 43-44].

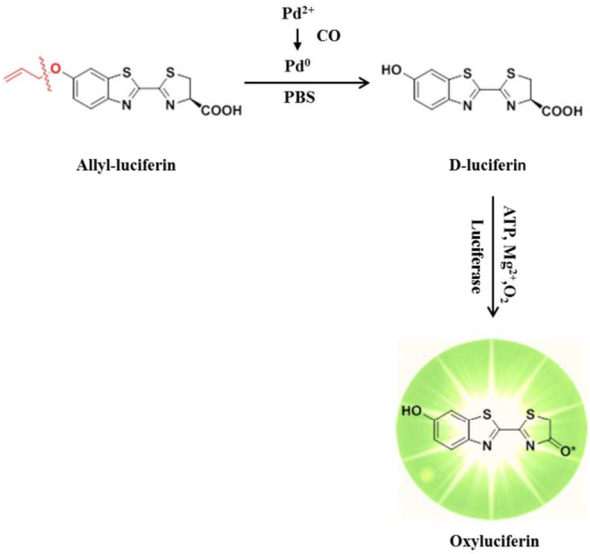

Scheme 1. The proposed sensing mechanism for bioluminescence detection of CO by a new probe allyl-luciferin via Pd^0-mediated Tsuji-Trost reaction.

EXPERIMENTAL SECTION

Materials and Instruments:

Millipore water was used throughout the analytical experiments. The bioluminescence spectra were determined with an IVIS Kinetic (Caliper Life Sciences, USA) equipped with a cooled charge coupled device (CCD) camera for bioluminescent imaging of the cells and nude mice. TLC plates were employed for monitoring a reaction progress with UV light (254 and 365 nm). All NMR data was taken on a 600 MHz spectrometer (Bruker Co., Ltd., Germany). Mass spectra were recorded on an Agilent 1100 LC/MS system. Luciferase was obtained from Promega. Heme and ATP were bought from Sigma-Aldrich. CORM-3 was purchased from Target Molecule Corp.

Synthesis of Allyl-CBT: 2-Cyano-6-hydrocybenzothiazole (150 mg, 0.85 mmol) was placed in DMF and K_2CO_3 (352.4 mg, 2.55 mol), as a base, was added into the reaction solution. After the mixture was stirred at room temperature for 15 min, allyl bromide (369 µL, 4.26 mmol) was added and the temperature of the mixture was heated to 70 ℃ for overnight. As the completion of the reaction under TLC monitoring, the reaction mixture was diluted with ethyl acetate after cool down and washed with saturated salt water for three times. The organic phase was dried over anhydrous magnesium sulfate, the solvent was then removed under reduced pressure and the crude solid product was purified via semi-prepared silica gel plate (petroleum ether: ethyl acetate = 3:1, v/v) to afford allyl-CBT as a white solid (150.6 mg, yield 82 %).^{1}H NMR (600 MHz, $CDCl_3$) δ = 8.07 (d, J=9.1, 1H), 7.36 (d, J=2.5, 1H), 7.26 (dd, J=9.1, 4.6, 1H), 6.09 (ddt, J=17.2, 10.5, 5.3, 1H), 5.47 (ddd, J=17.3, 3.0, 1.5, 1H), 5.37 (dq, J=10.5, 1.3,1H), 4.65 (dt, J=5.3, 1.5, 2H). ^{13}C NMR (151 MHz, $CDCl_3$) δ = 159.5, 147.0, 137.5, 133.5, 132.3, 126.0, 119.0, 118.7, 113.4, 104.2, 69.7. $C_{11}H_8N_2OS$ $[M + H]^+$ calcd. 217.0, found 217.0.

Synthesis of Allyl-luciferin: Allyl-luciferin was synthesized according to a modified literature procedure[45]. D-Cysteine hydrochloride monohydrate (184.4 mg, 1.05 mmol) was charged in PBS buffer (10 mM pH 7.4). 150.6 mg of allyl-CBT (0.70 mmol) was placed in dichloromethane and methanol (dichloromethane / methanol =1/5.5, V/V), and then, the above-prepared D-cysteine hydrochloride monohydrate solution was slowly added into the allyl-CBT solution. After the reaction mixture was refluxed at 50℃ for overnight, the solvent was then removed under reduced pressure and the crude solid product was purified using reverse-phase preparative-HPLC (Dikma C_{18} column 250*10.0mm, 5 µm, using a isocratic run of MeCN (38 %) and 0.1 % aqueous trifluoroacetic acid (TFA) at 4.5 mL/min) to provide the desired compound (69.4 mg, yield 31 %). ^{1}H NMR (600 MHz, MeOD) δ = 7.98 (d, J=9.0, 1H), 7.57 (d, J=2.4, 1H), 7.22 (dd, J=9.0, 2.5, 1H), 6.12 (ddd, J=22.4, 10.5, 5.2, 1H), 5.47 (dd, J=17.3, 1.6, 1H), 5.41 (t, J=9.0, 1H), 5.31 (dd, J=10.6, 1.4, 1H), 4.67 (d, J=5.2, 2H), 3.78 (m, 2H). ^{13}C NMR (151 MHz, MeOD) δ = 173.5, 167.8, δ = 160.0, 159.7, 149.1, 139.2, 134.5, 126.0, 118.8, 118.2, 106.2, 79.7, 70.6, 36.0. $C_{14}H_{12}N_2O_3S_2$ $[M + H]^+$ calcd. 321.0, found 321.0.

The Kinetics of Allyl-luciferin in Bulk PBS: Because of its poor solubility in water, allyl-luciferin was prepared in DMSO solution. Then the probe was diluted with PBS buffer (10 mM pH 7.4). The reaction of allyl-luciferin and $PdCl_2$ (100 µM each) with CORM-3 (100 µM) was started in PBS buffer. As a blank control experiment, PBS buffer was employed instead of CORM-3 solution. The above reactions (100 µL) were carried out at room temperature in the dark for 0, 5, 10, 15, 20, 25, 30, 35, 40, 45, 50 and 55 min, respectively, followed by 1 µL (100 mM) of ATP and 2 µL (100 µg/mL) of luciferase for each tube. BL measurement was carried out with a BPCL chemiluminescence analyzer (Beijing, China). BL signal for each tube was reported in photons per second.

Selectivity Measurement: The mixture solutions (100 µL) of allyl-luciferin and $PdCl_2$ (100 µM each) were reacted

with the same concentration of analytes (100 μM each), including $NaHCO_3$, NaHS, Na_2SO_4, Na_2CO_3, $NaNO_2$, $Na_2S_2O_3$, Na_2SO_3, cysteine (Cys), glutathione (GSH), NaF, $NaNO_3$, NaAc, $NaHSO_4$, KI, NaClO, tert-butyl hydroperoxide (t-BuOOH), NO, H_2O_2 and CORM-3 in PBS buffer. The reactions were carried out at room temperature without light for 15 min, followed by 1 μL of ATP (100 mM) and 2 μL of luciferase (100 μg/mL) for each tube. BL signal for each tube was reported in photons per second.

Sensitivity Measurement: The mixture solutions (100 μL) of allyl-luciferin and $PdCl_2$ (100 μM each), were respectively incubated with series concentrations of CORM-3 in PBS buffer. As a blank control, a same volume of PBS was added to the mixture solution of allyl-luciferin and $PdCl_2$ (100 μM) instead of CORM-3. The blank control and sample reactions were carried out at room temperature without light for 15 min, followed by 1 μL of ATP (100 mM) and 2 μL of luciferase (100 μg/mL) for each tube. BL signal for each tube was reported in photons per second.

The Toxicity Analysis of Allyl-luciferin, $PdCl_2$ and $PdCl_2$-containing Liposomes: Cell viability was assessed by 3-(4, 5-dimethyl-2-thiazolyl)-2, 5-diphenyltetrazolium bromide in HEK 293T cell line. HEK 293T cells were grown in Gibco DMEM supplemented with 10 % FBS, 1 % streptomycin and 1 % penicillin. Cells were seeded onto white 96-well plates (5000 cells per well) and incubated to ~80 % density. Following that, various concentrations of allyl-luciferin, $PdCl_2$ and $PdCl_2$-containing liposomes (0, 0.1, 1, 10, 25, 50, 100, 250 and 500 μM) were placed into each well, respectively. After 12 h of treatment at 37 ℃, 10 μL of CCK8 solution was added into each well. After 2 h incubation, absorbance of the solution was then measured at 450 nm with a microplate reader.

Bioluminescence Imaging of CORM-3-triggered Exogenous CO in Cells: Huh7 cells and MDA-MB-231 cells were grown in Gibco DMEM supplemented with 10 % FBS, 1 % streptomycin and 1 % penicillin. Cells were seeded into 35 mm glass bottom dishes for 24 h incubation to render the confluence up to around 80%. Equal volume of cells were charged into black 96-well plates (5×10^5 cells per well). Series concentrations of CORM-3 (0 - 1500 μM) were incubated with Huh7 cells and MDA-MB-231 cells for 10 min. Following that, allyl-luciferin and $PdCl_2$ (100 μM each) were immediately added into the plates and incubated for 40 min. Bioluminescence signal (photons per second) was immediately measured for 30 s using a Xenogeny IVIS spectrum imaging system (Camera Temp: -80℃; Stage Temp: 30℃; Excitation Filter: Block; Emission Filter: Open).

Bioluminescence Imaging of Heme-triggered Endogenous CO in Cells: Huh7 cells and MDA-MB-231 cells were grown in Gibco DMEM supplemented with 10 % FBS, 1 % streptomycin and 1 % penicillin. Then, the cells were seeded onto black 96-well plates (5×10^5 cells per well) and allowed to grow for overnight at 37 ℃ in a 5 % CO_2 humid incubator. Following that, the heme (200, 300 and 400 μM) was added into the wells, as a vehicle control, equal volume of PBS buffer was added into relative wells instead of heme. After 1 h incubation, the DMEM was removed from the chambers containing cells and was washed with PBS buffer. The cells in the bottom of wells were finally covered in PBS buffer, simultaneously. Then, allyl-luciferin and the $PdCl_2$-containing liposomes (100 μM each) were added into the corresponding wells and incubated for about 2 h prior to imaging.

Bioluminescence Imaging of Exogenous CO in Mice: On the first day, we choose two nude mice, 200 μL of ally-luciferin (5 mM with 40% DMSO) and 50 μL of $PdCl_2$-containing liposomes were intraperitoneally and intratumorally injected into each nude mouse as control groups. BL imaging was captured for 60 s using the IVIS Imager. On the second day, the same mice received 200 μL of ally-luciferin (5 mM) and then an intraperitoneal injection of 50 μL CORM-3 (10 and 15 mM), followed by an intratumoral injection of 50 μL PdCl2-containing liposomes (100 μM) for each mouse. BL imaging was also measured for 60 s by the IVIS Imager.

Bioluminescence Imaging of Endogenous CO in Mice: On the first day, we choose another two nude mice, 200 μL of allyl-luciferin (5 mM) and 50 μL of PdCl2-containing liposomes were intraperitoneally and intratumorally injected into each nude mouse as control groups, respectively. BL imaging was then measured for 60 s using the IVIS Imager. On the second day, the same mice received an intraperitoneal injection of 50 μL heme (20 and 40 mM). After 3 h, 200 μL of allyl-luciferin (5 mM) was injected intraperitoneally into the mice, and then 50 μL PdCl2-containing liposomes (100 μM) was intratumorally injected for each mouse. BL imaging was also measured for 60 s by the IVIS Imager.

RESULTS AND DISCUSSION

Synthesis:

Our initial study began with the introduction of functional reaction site: Allyl bromide was reacted with commercially available starting material (6`-hydroxyl of 2-cyano-6-hydroxybenzothiazole) through Williamson ether synthesis as shown in Figure 1. Then a cyclization reaction could spontaneously proceed between D-cysteine hydrochloride monohydrate and allyl-CBT in methanol and PBS buffer (10 mM pH 7.4) to obtain allyl-luciferin. The details of synthesis can be found in the Experimental Section and the structures of allyl-CBT and allyl-luciferin were confirmed by ESI-MS and ^{1}H NMR and ^{13}C NMR spectroscopy (See supporting information Figures S4-9).

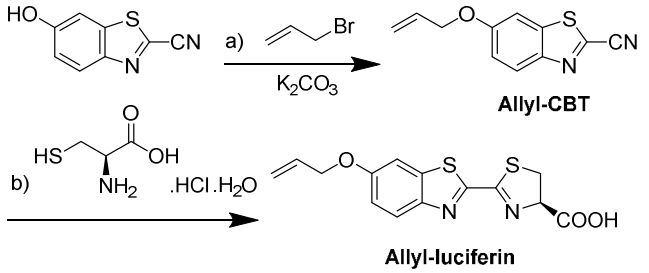

Figure 1. Synthesis of allyl-luciferin. (a) allyl bromide (5.0 equiv), K_2CO_3 (3.0 equiv), DMF, 70℃, overnight, 82 %. (b) H-D-Cys-OH • HCl • H_2O (1.5equiv), 50℃, overnight, 31 %.

The Kinetics of Allyl-luciferin in Bulk PBS: With allyl-luciferin in hand, we tested its BL properties and CO reactivity in PBS buffer. For in vitro analysis, a commercially available and water soluble complex CORM-3 was utilized as an easy-to-hand CO-releasing molecule[2-3, 29, 34-37,43-44,46-47] (1 mole of CORM-3 can produce 1 mole of CO on the basis of previous reports[2, 29, 46]). As expected, the modification of allyl on the D-luciferin backbone rendering the molecules incapable of interacting with luciferase to produce light. A robust turn-on BL response was triggered, only after the addition of 100 μM CORM-3 into a solution of allyl-luciferin in the presence of firefly luciferase, ATP and 100 μM $PdCl_2$ via CO-induced Pd^0-mediated Tsuji-Trost reaction. On the basis of the encouraging results, time-dependent BL responses of allyl-luciferin to CO were evaluated in PBS buffer by comparing the net BL intensity, where the net BL intensity was defined as (BL intensity–BL_0 intensity), BL intensity represents the total flux of samples and BL_0 intensity represents the blank total flux. As shown in Figure 2, kinetic experiments exhibited that one 15-min reaction was optimum between allyl-luciferin and CORM-3 in PBS solution.

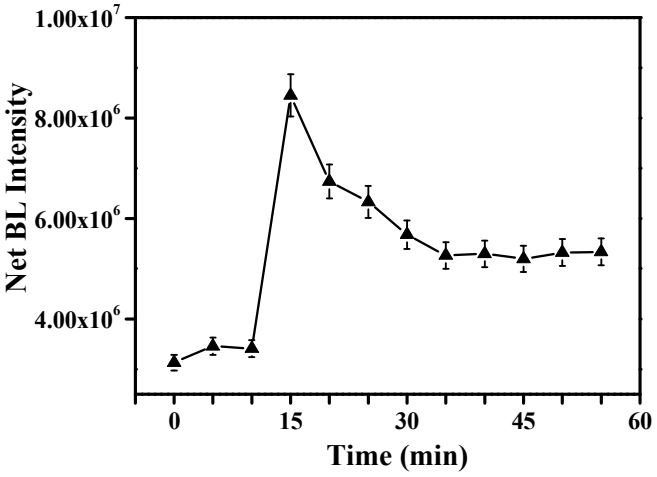

Figure 2. Bioluminescence time-dependence of allyl-luciferin, $PdCl_2$ with CORM-3 (allyl-luciferin, $PdCl_2$ and CORM-3, 100 μM each;) in PBS buffer (10 mM, pH 7.4) at room temperature without light for 0, 5, 10, 15, 20, 25, 30, 35, 40, 45, 50 and 55 min, then 1 μL (100 mM) of ATP and 2 μL (100 μg/mL) of luciferase were added respectively.

Selectivity Measurement: The selectivity of allyl-luciferin was tested by comparing BL intensities among allyl-luciferin and bioactive small molecules such as reactive nitrogen, oxygen, and sulfur species, including $NaHCO_3$, NaHS, Na_2SO_4, Na_2CO_3, $NaNO_2$, $Na_2S_2O_3$, Na_2SO_3, Cys, GSH, NaF, $NaNO_3$, NaCl, NaAc, $NaHSO_4$, KI, NaClO, t-BuOOH, NO, H_2O_2 and CORM-3 in PBS buffer. To our delight, as depicted in Figure 3, the turn-on BL response for allyl-luciferin was found to have excellent selectivity for capturing CO over other substances, due to that the selective recognition of CO by allyl-luciferin is based on CO-induced Pd^0-mediated Tsuji-Trost reaction. However, other testing species almost did not trigger BL responses, which may be due to that these molecules can't reduce $PdCl_2$ to Pd^0.

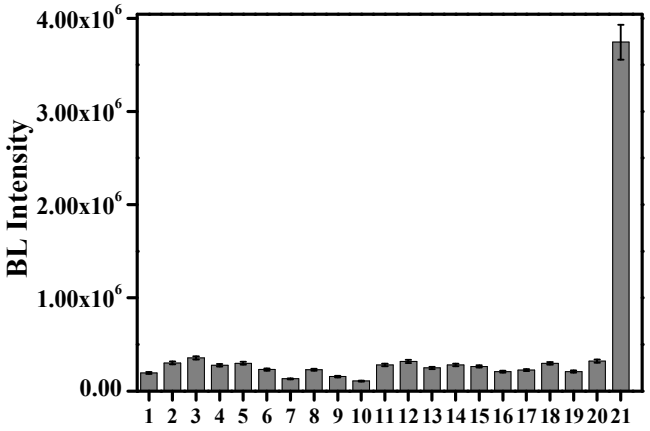

Figure 3. Bioluminescence changes of allyl-luciferin and $PdCl_2$ (100 μM each) with other bioactive small molecules (100 μM each) in PBS (10 mM, pH 7.4): 1, PBS; 2, $NaHCO_3$; 3, NaHS; 4, Na_2SO_4; 5, Na_2CO_3; 6, $NaNO_2$; 7, $Na_2S_2O_3$; 8, Na_2SO_3; 9, Cys; 10, GSH; 11, NaF; 12, $NaNO_3$; 13, NaCl; 14, NaAc; 15, $NaHSO_4$; 16, KI; 17,NaClO; 18, t-BuOOH; 19,NO; 20, H_2O_2; 21, CORM-3. Other experimental parameters such as the reaction temperature, reaction time, amounts of ATP and luciferase were the same as described in Figure 2.

Sensitivity Measurement: It is well known that the sensitivity of a new probe is a key performance indicator. On the basis of the 3σ method, a detection limit for CORM-3 was calculated to be about 58 nM and also good correlations (R^2=0.9828) were observed between the net BL intensity and CORM-3 concentrations from 0.1 to 250 μM (Figure 4). Overall, allyl-luciferin may be employed as an effective tool for monitoring intracellular CO, which is comparable or even better than most reported fluorescent probes [2, 35, 37].

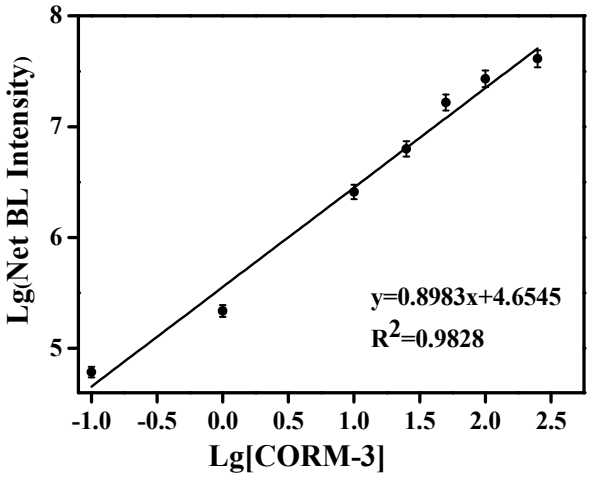

Figure 4. Calibration curve of the net BL intensity vs. the concentration of CORM-3. Other experimental parameters such as the concentrations of allyl-luciferin and $PdCl_2$, the reaction temperature, reaction time, amounts of ATP and luciferase were the same as described in Figure 2.

The Toxicity Analysis of Allyl-luciferin, $PdCl_2$ and $PdCl_2$-containing Liposomes: To employ allyl-luciferin for the detection of CO in living cells, a key question is whether the cells will survive during living cell imaging. Therefore, the cytotoxicity of allyl-luciferin, $PdCl_2$ and $PdCl_2$-containing liposomes were evaluated by the CCK8 assay. Figures 5a, 5b and 5c showed that cell viability remained constant over the evaluated concentration range of allyl-luciferin, $PdCl_2$ and $PdCl_2$-containing liposomes.

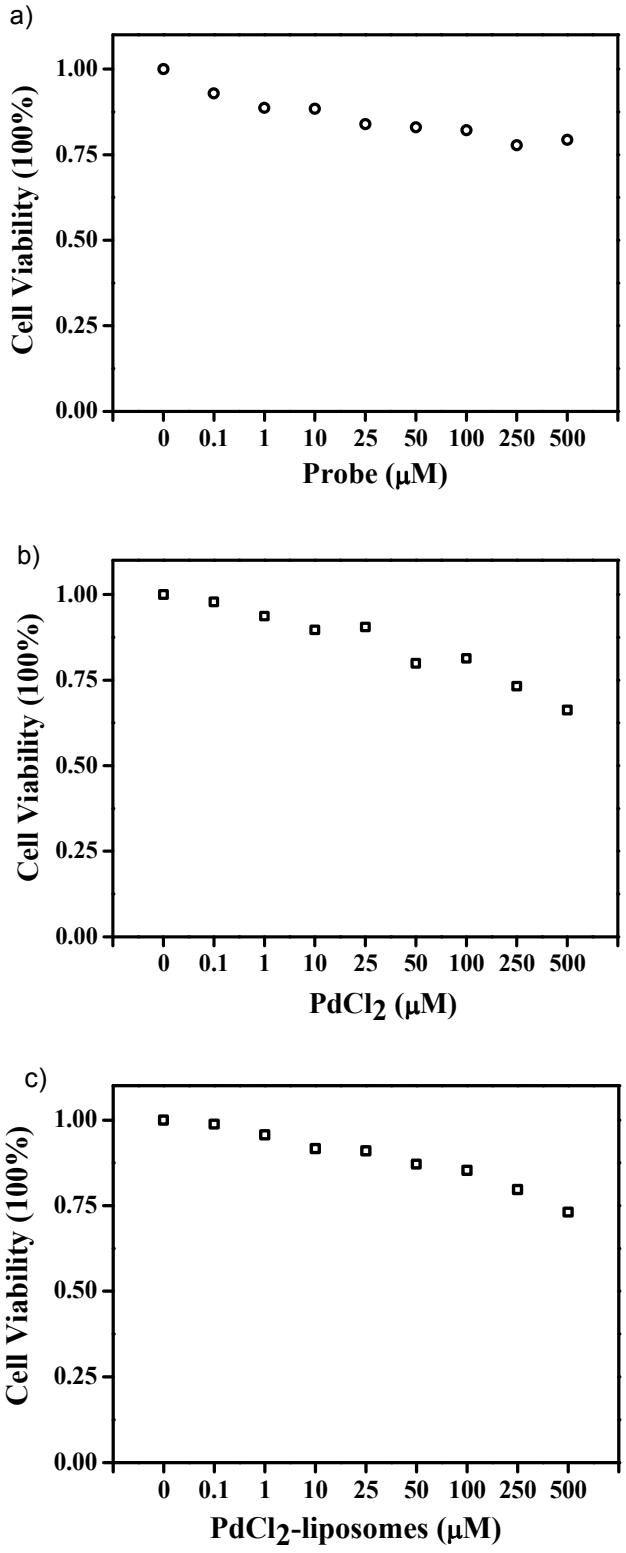

Figure 5. (a) CCK8 assay for the viability of HEK 293T cell treated with various concentrations (0-500 μM) of allyl-luciferin.. (b) CCK8 assay for the viability of HEK 293T cell treated with various concentrations (0-500 μM) of PdCl2.. (c) CCK8 assay for the viability of HEK 293T cell treated with various concentrations (0-500 μM) of PdCl2-containing liposomes.

Bioluminescence Imaging of CORM-3-triggered Exogenous CO in Cells: We then sought to evaluate the ability of allyl-luciferin to serve as BL agent for imaging CO inside living cells. Huh7 cells and MDA-MB-231 cells were selected to incubate with various concentrations of CORM-3 respectively and then the cells were treated with allyl-luciferin in the presence of 100 μM $PdCl_2$ in the black 96-well plates. Data was acquired using a Xenogeny IVIS Spectrum imaging system. A bright BL cell images was found to be dependent on the concentration of CORM-3 (0-1500 μM) and 50 μM of CORM-3 was clearly seen in both Huh7 cells (Figures 6a and 6b) and MDA-MB-231 cells (Figure S2). These results clearly demonstrated that allyl-luciferin was suitable for the visualization of exogenous CO in living cells by using BL imaging technique.

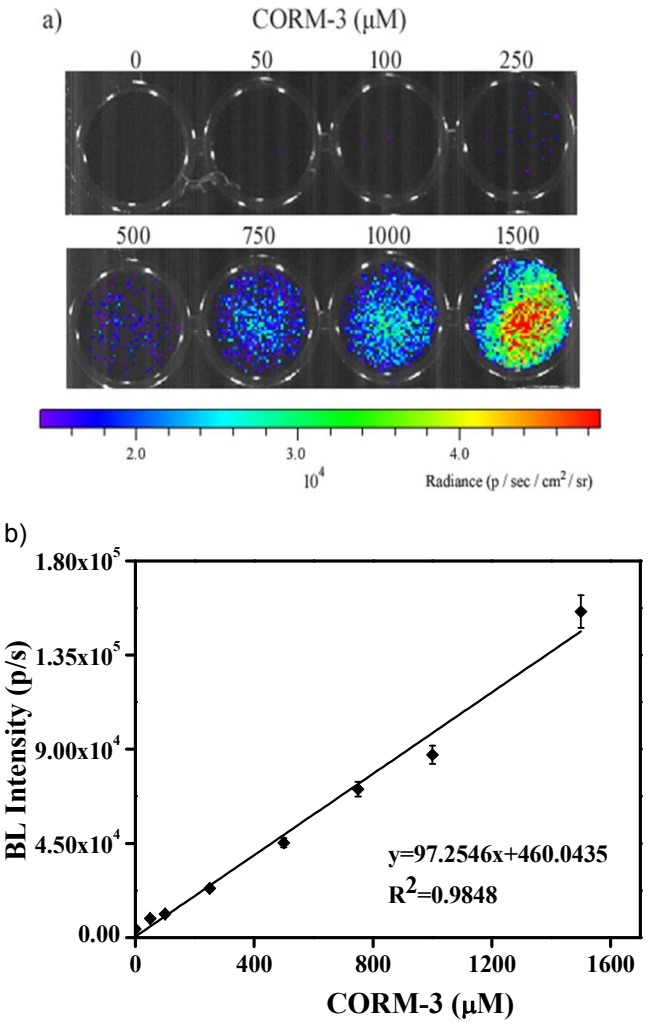

Figure 6. Bioluminescence images of CORM-3 triggered CO in luciferase-transfected Huh7 cells. (a) Various concentrations of CORM-3 (0 - 1500 μM) were incubated with Huh7 cells for 10 min. Then, allyl-luciferin and $PdCl_2$ (100 μM each) were added and incubated for 40 min. Images was measured using a Xenogeny IVIS spectrum imaging system. (b) Calibration curve of BL intensity vs. CORM-3 concentrations (0 - 1500 μM).

Bioluminescence Imaging of Heme-triggered Endogenous CO in Cells: To our knowledge, endogenous CO can be generated via the interaction of heme and heme oxygenases (HOS) [4-6, 48-49]. Therefore, our major concern was whether allyl-luciferin has capability to detect endogenously produced CO. Both Huh7 cells and MDA-MB-231 cells were seeded onto the black 96-well plates overnight. Then 10 μL of heme (200, 300 and 400 μM) and PBS were pre-incubated with these cells for 1 h, respectively, and both Huh7 cells and MDA-MB-231 cells were added allyl-luciferin and also $PdCl_2$ for 2 h after washing with PBS buffer. However, no apparent BL signal was found, and thus we speculated that the main reasons may be possibly due to the following three factors, (1) the endogenously produced CO that stimulated with heme is supposed to be quite low; (2) $PdCl_2$ has poor membrane permeability; (3) the cells were pre-washed to remove any interference from complex matrix before imaging endogenous CO with PBS buffer, leading to that those remaining attached cells in the bottom of 96-well plates were much less than 5×10^5 cells and could not emit enough BL signals. Since it is unable to further increase the attached cells, and thus we expected to increase the membrane permeability of $PdCl_2$ through the use of the $PdCl_2$-containing liposomes instead of free $PdCl_2$. The liposomes have an aqueous PdCl2 core surrounded by a hydrophobic lipid membrane. The liposome bilayer can fuse with the cell membrane, thus delivering PdCl2 to enter the cell according to "like dissolves like". As expected, a clear and distinguishing BL images were observed after using the $PdCl_2$-containing liposomes instead of free PdCl2 for imaging exogenous CO (Figure S3), which proved that improving the membrane permeability of $PdCl_2$ may be a good way for BL imaging of the endogenously produced CO in living cells. As we can see, the levels of endogenous CO of Huh7 cells (Figures 7a and 7b) and MDA-MB-231 cells (Figures 7c and 7d) were increased with the incubation of heme, since the BL in the presence of heme were higher than that of PBS control group, where the BL ratio was defined as (BL intensity/BL_0 intensity). Therefore, all data definitely indicated that allyl-luciferin is promising as an effective tool for monitoring endogenously produced CO.

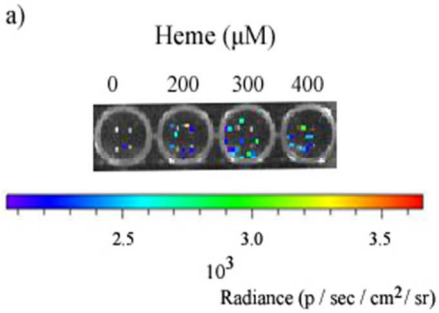

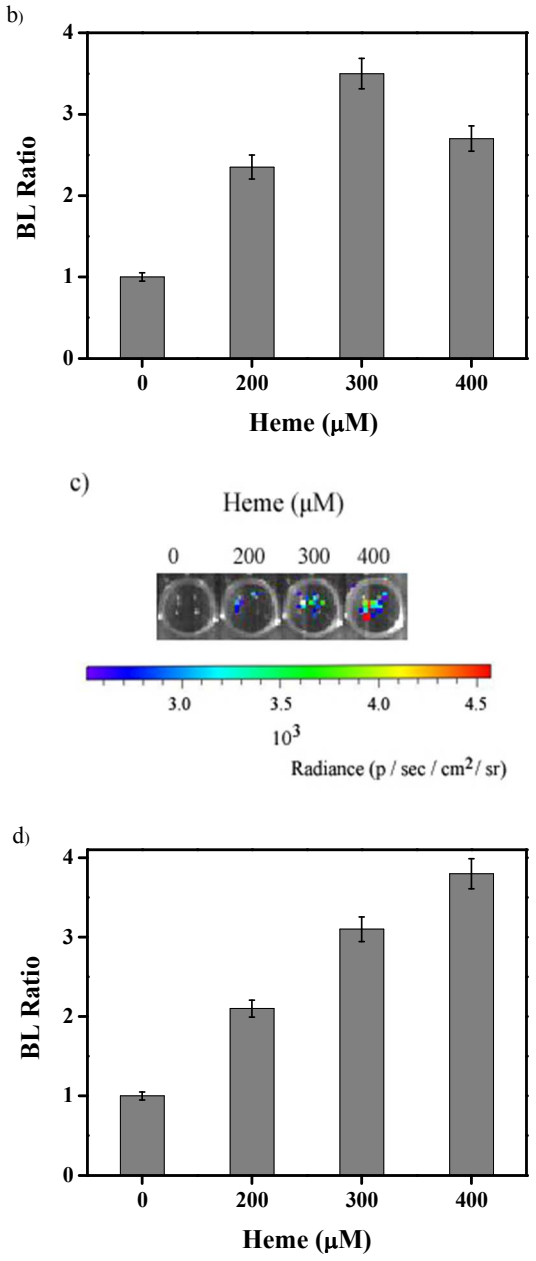

Figure 7. Bioluminescence images of heme-triggered endogenous CO in luciferase-transfected Huh7 and MDA-MB-231 cells. The cells were treated with heme and PBS for about 1 h. Then, allyl-luciferin and the PdCl2-containing liposomes (100 μM each) were added and incubated for 2 h. Images was measured using a Xenogeny IVIS spectrum imaging system. (a) BL images acquired from Huh7 cells treated with heme (200, 300 and 400 μM) and PBS. (b) BL ratio was measured from Huh7 cells treated with heme and PBS. (c) BL images acquired from MDA-MB-231 cells treated with heme (200, 300 and 400 μM) and PBS. (d) BL ratio was measured from MDA-MB-231 cells treated with heme and PBS.

Bioluminescence Imaging of Exogenous CO in Mice: Based on the above studies, we explored the capability of allyl-luciferin for exogenous CO visualization in vivo. Hence, a luciferase-transfected Huh7 tumor was xenografted in the right forelimb of each nude mouse. Due to individual differences in mice, the size and shape of tumors are often different for different mouse, and thus the same mouse was used as its own control. As shown in Figure 8, compared with the blank control, BL signals from treated CORM-3 groups were obviously enhanced. These results suggested that allyl-luciferin was applicable for imaging exogenous CO activity in tumors in living mice.

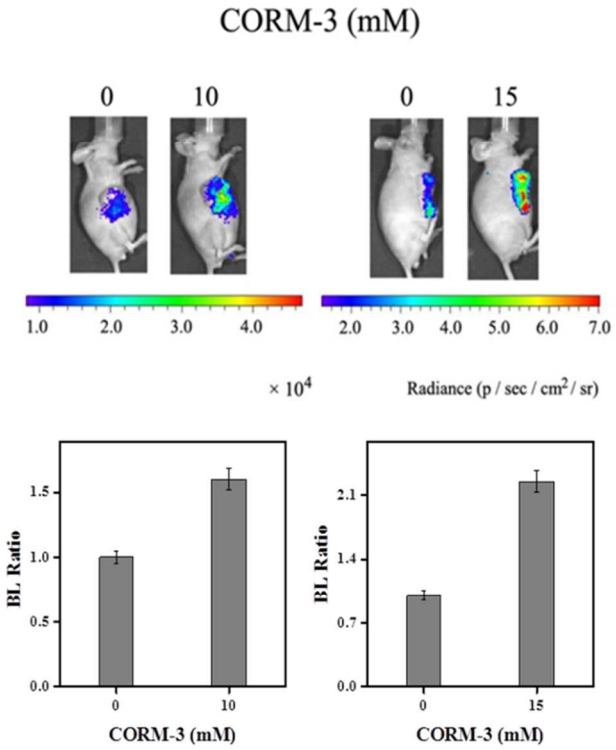

Figure 8. Bioluminescence imaging of nude mice that xenografted with luciferase-transfected Huh7 tumors. The images obtained from two nude mice treated with different concentrations of CORM-3 (10 and 15 mM) and BL ratio were also measured from each mouse that treated-CORM-3 group and the relative control group.

Bioluminescence Imaging of Endogenous CO in Mice: After receiving an injection of allyl-luciferin and PdCl2-containing liposomes, mice only displayed a weak BL in the xenografted liver tumors. In contrast, BL signals (Figure 9) exhibited an obvious increase after incubation with heme compared with the control group, demonstrating that allyl-luciferin could even detect endogenous CO *in vivo*. However, we should state that this in vivo CO imaging is only partially successful, the maximum BL ratio values of the probe were comparatively not high especially for endogenous CO in intact living mice, more work still needs to be done to improve the probe for endogeous CO imaging in mice.

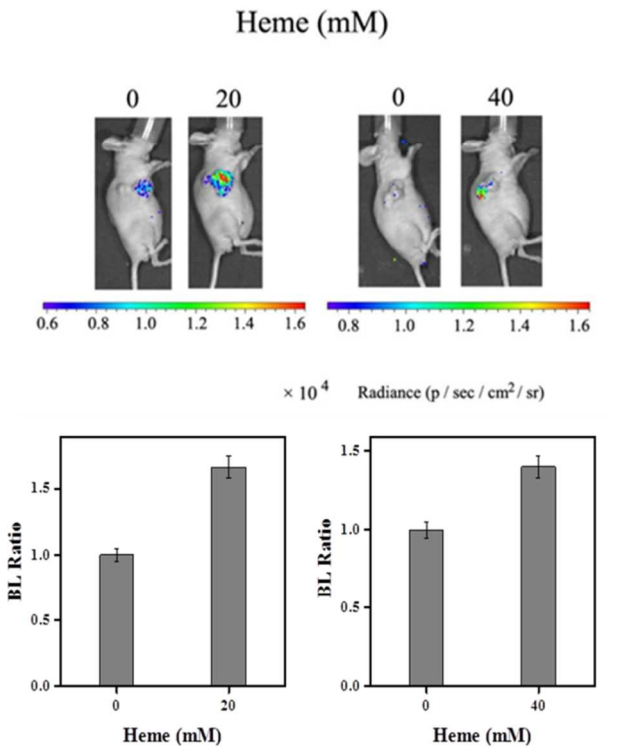

Figure 9. Bioluminescence imaging of nude mice that xenografted with luciferase-transfected Huh7 tumors. The images obtained from another two nude mice treated with different concentrations of heme (20 and 40 mM) for 3 h and BL ratio were also measured from each mouse that treated-heme group and the relative control group.

CONCLUSION

In summary, we have successfully engineered and synthesized allyl-luciferin as a first new and promising BL imaging probe for real-time detection of CO. Notably, when compared to current CO fluorescent probes, the background interference of allyl-luciferin is eliminated and exhibited a clear turn-on BL response to CO that is selective over other biologically relevant analytes. Moreover, high sensitivity provides great advantages for imaging of exogenous and endogenous CO in cells and in nude mice, which may help us to explore practical applications for cancer diagnosis. In addition, data also showed that $PdCl_2$ has poor membrane permeability, which is detrimental to in vivo CO imaging. Through the use of the $PdCl_2$-containing liposomes, the membrane permeability of $PdCl_2$ can be greatly improved for successful imaging of endogenous CO. Further studies are also undertaken by designing new BL imaging probes for specific detection of CO in in intact living mice by integrating palladium moiety into a recognition unit.

ASSOCIATED CONTENT

Supporting Information

Supplementary experimental methods, probes characterization are available free of charge via the Internet at http://pubs.acs.org."

AUTHOR INFORMATION

Corresponding Author

*jzlu@shmu.edu.cn.

Notes

The authors declare no competing financial interest.

ACKNOWLEDGMENT

This work was supported by the Natural Science Foundation of China (No. 21675030).

REFERENCES

(1) Heinemann, S. H.; Hoshi, T.; Westerhausen, M.; Schiller, A., *Chem. Commun*. **2014**, *50*, 3644-3660.

(2) Michel, B. W.; Lippert, A. R.; Chang, C. J., *J. Am. Chem. Soc*. **2012**, *134*, 15668-15671.

(3) Li, Y.; Wang, X.; Yang, J.; Xie, X.; Li, M.; Niu, J.; Tong, L.; Tang, B., *Anal. Chem*. **2016**, *88*, 11154–11159.

(4) Maines, M. D., *FASEB J*. **1988**, *2*, 2557-2568.

(5) Ryter, S. W.; Alam, J.; Choi, A. M., *Physiol. Rev*. **2006**, *86*, 583-650.

(6) Tenhunen, R.; Marver, H. S.; Schmid, R., *Proc. Natl. Acad. Sci. U.S.A*. **1968**, *61*, 748–755.

(7) Bailey, T. S.; Pluth, M. D., *J. Am. Chem. Soc*. **2013**, *135*, 16697-16704.

(8) Kojima, H.; Hirotani, M.; Nakatsubo, N.; Kikuchi, K.; Urano, Y.; Higuchi, T.; Hirata, Y.; Nagano, T., *Anal. Chem*. **2001**, *73*, 1967-1973.

(9) Kojima, H.; Nakatsubo, N.; Kikuchi, K.; Kawahara, S.; Kirino, Y.; Nagoshi, H.; Hirata, Y.; Nagano, T., *Anal. Chem*. **1998**, *70*, 2446-2453.

(10) Lim, M. H.; Xu, D.; Lippard, S. J., *J. Nat. Chem. Biol*. **2006**, *2*, 375–380.

(11) Yang, Y.; Seidlits, S. K.; Adams, M. M.; Lynch, V. M.; Schmidt, C. E.; Anslyn, E. V.; Shear, J. B., *J. Am. Chem. Soc*. **2010**, *132*, 13114-13116.

(12) Henthorn, H. A.; Pluth, M. D., *J. Am. Chem. Soc*. **2016**, *137*, 15330–15336.

(13) Liu, C.; Pan, J.; Li, S.; Zhao, Y.; Wu, L. Y.; Berkman, C. E.; Whorton, A. R.; Xian, M., *Angew. Chem., Int. Ed*. **2011**, *50*, 10327-10329.

(14) Gahlaut, S. K.; Yadav, K.; Sharan, C.; Singh, J. P., *Anal. Chem*. **2017**, *89*, 13582-13588.

(15) Peng, H.; Cheng, Y.; Dai, C.; King, A. L.; Predmore, B. L.; Lefer, D. J.; Wang, B., *Angew. Chem., Int. Ed*. **2011**, *50*, 9672–9675.

(16) Qian, Y.; Karpus, J.; Kabil, O.; Zhang, S. Y.; Zhu, H. L.; Banerjee, R.; Zhao, J.; He, C., *Nat. Commun*. **2011**, *2*, 495-501.

(17) Sasakura, K.; Hanaoka, K.; Shibuya, N.; Mikami, Y.; Kimura, Y.; Komatsu, T.; Ueno, T.; Terai, T.; Kimura, H.; Nagano, T., *J. Am. Chem. Soc*. **2011**, *133*, 18003-18005.

(18) Tian, X.; Li, Z.; Lau, C.; Lu, J., *Anal. Chem*. **2015**, *87*, 11325-11331.

(19) Yu, F.; Li, P.; Song, P.; Wang, B.; Zhao, J.; Han, K., *Chem. Commun*. **2012**, *48*, 2852-2854.

(20) Bathoorn, E.; Slebos, D. J.; Postma, D. S.; Koeter, G. H.; van Oosterhout, A. J.; Van, d. T. M.; Boezen, H. M.; Kerstjens, H. A., *Eur. Respir. J*. **2007**, *30*, 1131-1137.

(21) Gu, Y. J.; Cheng, J.; Man, C. W.; Wong, W. T.; Cheng, S. H., *Nanomedicine*. **2012**, *8*, 204-211.

(22) Zhou, X.; Lee, S.; Xu, Z.; Yoon, J., *Chem. Rev*. **2015**, *115*, 7944-8000.

(23) Leffler, C. W.; Balabanova, L.; Fedinec, A. L.; Waters, C. M.; Parfenova, H., *J. Physiol. Heart Circ. Physiol.* **2003**, *285*, H74-H80.

(24) Qi, X.; Tcheranova, D.; Basuroy, S.; Parfenova, H.; Jaggar, J. H.; Leffler, C. W., *J. Physiol. Heart Circ. Physiol*. **2011**, *301*, H428–H33.

(25) Cao, Y.; Li, D. W.; Zhao, L. J.; Liu, X. Y.; Cao, X. M.; Long, Y. T., *Anal. Chem*. **2015**, *87*, 9696-9701.

(26) Kim, H. P.; Wang, X.; Nakao, A.; Kim, S. I.; Murase, N.; Choi, M. E.; Ryter, S. W.; Choi, A. M., *Proc. Natl. Acad. Sci. U. S. A*. **2005**, *102*, 11319-11324.

(27) Premkumar, D. R. D.; Smith, M. A.; Richey, P. L.; Petersen, R. B.; Castellani, R.; Kutty, R. K.; Wiggert, B.; Perry, G.; Kalaria, R. N., *J. Neurochem*. **1995**, *65*, 1399-1402.

(28) Raju, V. S.; Imai, N.; Liang, C. S., *J. Mol. Cell. Cardiol*. **1999**, *31*, 1581-1589.

(29) Feng, S.; Liu, D.; Feng, W.; Feng, G., *Anal. Chem*. **2017**, *89*, 3754-3760.

(30) Park, S. S.; Kim, J.; Lee, Y., *Anal. Chem*. **2012**, *84*, 1792-1796.

(31) Benito-Garagorri, D.; Puchberger, M.; Mereiter, K.; Kirchner, K., *Angew. Chem., Int. Ed*. **2008**, *47*, 9142-9145.

(32) Esteban, J.; Ros - Lis, J. V.; Marcos, M. D.; Moragues, M.; Soto, J.; Sancenón, F., *J. Am. Chem. Soc*. **2011**, *133*, 15762-15772.

(33) Heylen, S.; Martens, J. A., *Angew. Chem., Int. Ed*. **2010**, *49*, 7629-7630.

(34) Wang, J.; Karpus, J.; Zhao, B. S.; Luo, Z.; Chen, P. R.; He, C., *Angew. Chem., Int. Ed*. **2012**, *51*, 9652–9656.

(35) Pal, S.; Mukherjee, M.; Sen, B.; Mandal, S. K.; Lohar, S.; Chattopadhyay, P.; Dhara, K., *Chem. Commun*. **2015**, *51*, 4410-4413.

(36) Xu, Z.; Yan, J.; Li, J.; Yao, P.; Tan, J.; Zhang, L., *Tetrahedron Lett*. **2016**, *57*, 2927-2930.

(37) Zheng, K.; Lin, W.; Tan, L.; Chen, H.; Cui, H., *Chem. Sci*. **2014**, *5*, 3439-3448.

(38) Gao, Y.; Lin, Y.; Liu, T.; Chen, H.; Yang, X.; Tian, C.; Du, L.; Li, M., *Anal. Chem*. **2017**, *89*, 12488–12493.

(39) Hananya, N.; Shabat, D., *Angew. Chem. Int. Ed*. **2017**, *56*, 2-12.

(40) Roth-Konforti, M.; Bauer, C.; Shabat, D., *Angew.Chem. Int. Ed*. **2017**, *56* ,15633–15638.

(41) Wu, W.; Li, J.; Chen, L.; Ma, Z.; Zhang, W.; Liu, Z.; Cheng, Y.; Du, L.; Li, M., *Anal. Chem.* **2014**, *86*, 9800-9806.

(42) Ke, B.; Wu, W.; Wei, L.; Wu, F.; Chen, G.; He, G.; Li, M., *Anal. Chem*. **2015**, *87*, 9110-9113.

(43) Feng, W.; Liu, D.; Feng, S.; Feng, G., Anal. Chem. 2016, 88, 10648–10653.

(44) Feng, W.; Liu, D.; Zhai, Q.; Feng, G., *Sens. Actuators B*. **2017**, *240*, 625-630.

(45)White, E. H.; Wörther, H.; Seliger, H. H.; Mcelroy, W. D., *J. Am. Chem. Soc*. **1966**, *88*, 2015-2019.

(46) Clark, J. E.; Naughton, P.; Shurey, S.; Green, C. J.; Johnson, T. R.; Mann, B. E.; Foresti, R.; Motterlini, R., *Circ. Res*. **2003**, *93*, 2-8.

(47) Motterlini, R.; Mann, B. E.; Johnson, T. R.; Clark, J. E.; Foresti, R.; Green, C. J., *J. Curr. Pharm. Des*. **2003**, *9*, 2525-2539.

(48) Xuan, W.; Zhu, F. Y.; Xu, S.; Huang, B. K.; Ling, T. F.; Qi, J. Y.; Ye, M. B.; Shen, W. B., *Plant Physiol*. **2008**, *148*, 881-893.

(49) Liu, K.; Kong, X.; Ma, Y.; Lin, W., *Angew. Chem., Int. Ed*. **2017**, *56*, 13489–13492.

for TOC only